Available online at BCREC website: https://bcrec.id

Bulletin of Chemical Reaction Engineering & Catalysis, 17 (4) 2022, 831-838

Research Article

Synthesis of Mesoporous Silica Incorporated with Low Iron Concentration and Gelatin Co-Template via The Ultrasonication Method and Its Methylene Blue Photodegradation Performance

Maria Ulfa*, Sandini Ajeng Istanti

Chemistry Education Study Program, Faculty of Teacher Training and Education, Sebelas Maret University, Surakarta 57126, Central Java, Indonesia.

Received: 19th October 2022; Revised: 18th November 2022; Accepted: 28th November 2022
Available online: 6th December 2022; Published regularly: December 2022

Abstract

In this work, low iron concentration incorporated on mesoporous silica with gelatin co-template (Fe_2O_3/GSBA-15) has been successfully synthesized via the ultrasonication method. The physical, chemical, and structural properties of the samples were investigated with X-Ray Diffraction (XRD), Scanning Electron Microscope- Energy Dispersive X-Ray (SEM-EDX), Fourier Transform Infra-Red (FTIR), and N_2 adsorption-desorption. Results showed good distribution of low concentration of iron oxide on the gelatin mesoporous silica GSBA-15. Elemental and surface analysis presented that iron oxide incorporation with higher concentration exhibited lower surface area due to the blocking pore. The highest photocatalytic activity on the methylene blue dye degradation was achieved at 10% Fe_2O_3/GSBA-15 with ~80% efficiency. The results revealed that the photocatalytic activity of Fe_2O_3/GSBA-15 enhanced with the presence of iron oxide.

Keywords: Mesoporous silica; iron oxide; gelatin; incorporation; ultrasonication; photocatalyst; methylene blue; photodegradation

How to Cite: M. Ulfa, S.A. Istanti. (2022). Synthesis of Mesoporous Silica Incorporated with Low Iron Concentration and Gelatin Co-Template via The Ultrasonication Method and Its Methylene Blue Photodegradation Performance. *Bulletin of Chemical Reaction Engineering & Catalysis*, 17(4), 831-838 (doi: 10.9767/bcrec.17.4.16210.831-838)

Permalink/DOI: https://doi.org/10.9767/bcrec.17.4.16210.831-838

1. Introduction

Methylene blue (MB) is a liquid dye waste massively produced by the textile industry annually. MB waste enters the waters and poses many health risks [1]. MB waste is handled mainly through adsorption and photocatalysis [2,3]. The photocatalysis approach to reducing MB is famous as an environmentally friendly and high-efficiency method[4-6]. Many researchers have studied efficient photocatalysts to produce an effective photodegradation process. One of the photocatalysts reviewed is iron oxide [7,8]. However, the easy agglomeration of iron oxide causes high cost and low photocatalytic efficiency [9,10]. Therefore, a suitable support material is considered effective in increasing iron oxide distribution. Besides, the support material is attempted to be synthesized from various materials that have high sustainability by minimizing synthetic materials, for example, with gelatin as the co-template [11-14]. The main problem is that the normal impregnation process still causes a large metal oxide agglomeration effect, reducing the photocatalytic efficien-

* Corresponding Author.
Email: ulfa.maria2015@gmail.com; mariaulfa@staff.uns.ac.id (M. Ulfa)

cy. Hence, various impregnation modifications have been performed to deal with this problem so that metal oxides can be appropriately distributed, one of which is by the ultrasonication method [15-18].

The ultrasonication method is a simple synthesis pathway via a high-frequency sound field (>20 kHz). It is widely used in synthesizing organic and inorganic compounds because it is effective for homogenizing, mixing, and reducing particle size [16,19,20]. Ultrasonic waves have been used for the separation of agglomerates to make composites because they exhibit higher selectivity, reactivity, and improved product amount. Additionally, their energy savings are higher and cleaner than photochemical, hydrothermal, and pyrolysis [17,21,22].

However, the ultrasonication method has never been employed in the incorporation of iron oxide in mesoporous silica using gelatin as the co-template, especially at low concentrations of iron oxide. Thus, here, to prevent agglomeration and achieve better dispersion of iron oxide in silica, iron oxide precursors are impregnated on the silica surface via the ultrasonication method. Further, this research focuses on studying the effect of ultrasonication on iron oxide impregnation into mesopore silica with gelatin co-template. The synthesis results are characterized using XRD, SEM-EDS, FTIR, and Nitrogen (N_2) adsorption-desorption. The synthesis results are applied in methylene blue photocatalysis to determine information related to degradation efficiency and an appropriate kinetic model.

2. Materials and Methods

2.1 Synthesis of Fe_2O_3/GSBA-15

Mesopore silica with gelatin as the co-template (GSBA-15) was prepared by following the previous study with a P123:gelatin ratio of 1:0.01 (%w/w) [23]. The incorporation of iron oxide into GSBA-15 was done by mixing H_2O, $Fe(Cl)_6.6H_2O$, and GSBA-15 with a ratio of 2:10:100 (%w/v/w), respectively. It was then followed by ultrasonication at 100 rpm for 2 hours at a room temperature of 30 °C. The result was dried at 100 °C for 30 min and then activated with 0.5 M HCL, followed by calcination in a furnace at 600 °C for 6 hours. The resulting sample was named 1% Fe_2O_3/GSBA-15. The synthesis process was repeated for 5% and 10% concentration variations. Thus, there were three samples in this study, namely 1% Fe_2O_3/GSBA-15, 5% Fe_2O_3/GSBA-15, and 10% Fe_2O_3/GSBA-15.

2.2. Methylene Blue Photodegradation

The photocatalytic activity of Fe_2O_3/GSBA-15 was evaluated by methylene blue degradation. First, 200 mL of 5 ppm methylene blue solution was mixed into 50 mg Fe_2O_3/GSBA-15 photocatalyst. The solution was then irradiated under a UV lamp (300 W Xenon lamp at 365 nm). Samples were taken every 5 minutes of irradiation (until 90 minutes) and then measured by UV-Vis spectrophotometer at 665 nm (Shimadzu UV-3600) to determine the absorbance. Analysis of %Efficiency of methylene blue degradation was done using Equation (1).

$$\%Efficiency = \frac{C_0 - C_t}{C_0} x100\% \quad (1)$$

where, C_0 is the initial methylene blue concentration before irradiation, and C_t is the methylene blue concentration at t (min) after irradiation.

2.3. Characterization

Characterization was done using FTIR spectrophotometer (Nicolet 6700-Thermo Fisher Scientific), XRD (Philips X'pert, Cu-Ka 0.04° and counting time of per 10 s, 2θ 5–80°), SEM (ZEISS EVO MA and J-image (BSD-2 license) to count the number of particles, measure their size and calculate the average size of the SEM image data), and surface area analyzer (NOVA instruments© 1994–2010 Quantachrome Instruments version 11.0). The crystal size of gelatin mesoporous silica GSBA-15 and Fe_2O_3/GSBA-15 was calculated with the Debye Scherrer formula [23] as Equation 2.

$$D = \frac{0.9\lambda}{B\ cos\ \theta} \quad (2)$$

where, D is the crystal size, λ is the wavelength used in the XRD test (1.54056 Å), B is the half-peak width in radians, and θ is the angular position of the peak formation. Besides, the crystallinity of the sample [23] can also be calculated using Equation 3.

$$Crystallinity\ (\%) = \frac{Crystalline\ Area}{Amorphous\ Area} x100\% \quad (3)$$

3. Results and Discussion

Figure 1 shows that all samples have an amorphous silica phase at 2θ of 21.710° and 21.168°. While after impregnation, the peaks of Fe_2O_3 are visible at 2θ of 24.024°; 33.119°; 35.524°; 40.679°, 49.444°, 54.044°, 62.372°, and 63.905°. The peaks align with JCPDS database

#39-1346 [11]. The crystal size and crystallinity degree of gelatin mesoporous silica before and after 10% Fe_2O_3 impregnation change from 14% to 29% (Tabel 1). It indicates that the presence of iron oxide in the silica increases the crystal size and crystallinity.

Figure 2 presents the N_2 adsorption-desorption isotherm of mesoporous silica GSBA-15 before and after iron oxide incorporation. It exhibits that all samples have isotherm type IV with a hysteresis loop of type H-1 at a wide relative pressure (P/P_0) in the range of 0.5 to 0.8 and with almost vertical adsorption and desorption branches as a regular character of the mesoporous material. This type is in line with the previous report [24].

The surface area of the samples decreases from 481.7 m^2/g to 385.0 m^2/g after incorporating 10% iron oxide (Table 1). Besides, the pore volume also reduces from 0.62 cm^3/g to 0.585 cm^3/g due to pore clogging by iron oxide. The decrease in surface area after the incorporation of iron oxide in this study was only 18% which is much smaller than the previous study (43%). It is considered due to the ultrasonication effect homogenizing the distribution of iron oxide in the mesopore silica.

Figure 3 shows the FTIR spectra of gelatin mesoporous silica (GSBA-15) before and after the incorporation of iron oxide. It demonstrates

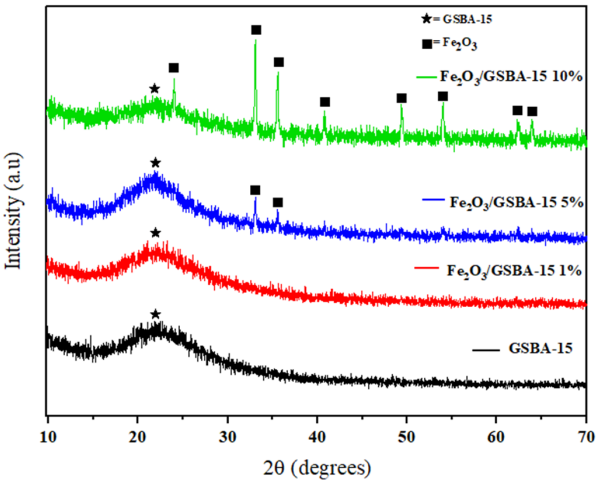

Figure 1. XRD of gelatin mesoporous silica (GSBA-15) before and after iron oxide incorporation

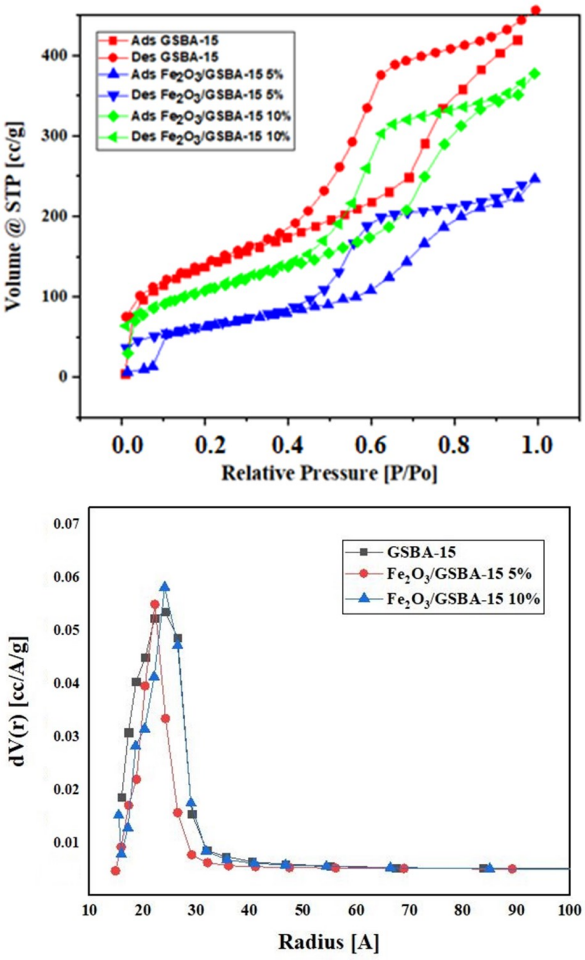

Figure 2. Nitrogen adsorption-desorption isotherm (top) and Pore size distribution (below) of mesoporous silica GSBA-15 before and after iron oxide incorporation

Table 1. Porosity, crystallinity, and element result

Sample	C (nm)	CD (%)	S_{BET} (m^2/g)	R (Å)	V (cm^3/g)	wt%	
						Si	Fe
GSBA-15	5.68	14.13	481.68	25.75	0.6204	41.57	-
1% Fe_2O_3/GSBA-15	7.87	16.18	Nd	Nd	nd	31.93	0.97
5% Fe_2O_3/GSBA-15	10.86	17.02	226.51	33.74	0.3822	30.74	1.58
10% Fe_2O_3/GSBA-15	27.91	28.76	385.01	30.39	0.5851	25.45	5.98

C: crystal size from XRD, CD: crystallinity degree from XRD, S_{BET}: surface area, V: pore volume, and R: pore radius from Nitrogen adsorption-desorption , %W: elemental weight from EDX

that there are absorption peaks of around 3400 cm^{-1} at the iron oxide concentrations of 5-10%, which is associated with the presence of water in Si–OH. All samples present absorption bands at 1108.71 and 870 $m^{-1,}$ indicating the stretching vibrations of Si–O–Si and Si–OH, respectively. Meanwhile, all samples with Fe_2O_3 incorporated exhibit an increasing absorption at 440 – 463 cm^{-1} as the representation of the presence of Fe–O.

Figure 4 depicts SEM images and particle size distribution of gelatin mesopores silica GSBA-15 before and after iron oxide incorporation. It reveals that the morphology of all mesopore silica samples is rod-shaped, with the particle size distribution between 354-757 nm. The morphology of all samples does not show significant aggregation of iron oxide. It is considered due to the ultrasonication effect, which helps distribute metal oxides on the silica surface. Nevertheless, the 10% iron oxide concentration decreases the particle size distribution. It might be because of silica shrinkage due to the intense attraction between Fe–O–Si on the surface.

Further, EDX analysis denotes that all samples experience an increase in Fe content after incorporating 1-10 % iron oxide. It has a Fe content of 0.97–5.98 % (Table 1). It indicates the success of the metal deposition process in mesopore silica by ultrasonication. Moreover, based on Figure 5, the increase in iron oxide content in mesoporous silica enhances the removal efficiency of methylene blue from 66% to 85% in 90 minutes of irradiation. It is considered due to the increase in well-dispersed catalytic sites, although in small levels, due to the effect of ultrasonication (Figure 5, Equations (1-5).

Further, this result can be compared with several previous studies using non-ultrasonic methods (see Table 2), which revealed that the incorporation of low iron content (< 30%) into the support material showed an efficiency of less than 50%, while high iron content between 35-65 % achieved an efficiency of 50-99 %. High iron content is not economical for large-scale photodegradation applications, so this is an important consideration in saving the environment. The research results using ultrasonication with metal oxides, but not iron oxides, reached 99% efficiency with an average irradiation time of 150-700 minutes. From this result, the ultrasonication method on the incorporation of iron oxide into the gelatin mesoporous silica G-SBA-15 provides many advantages in increasing the dispersion of small levels of Fe particles to the silica surface, which enhances the degradation efficiency of methylene blue significantly in the first 90 minutes. For the issue of saving the environment on a large scale, this gives cost and time efficiency advantages.

The mechanism of the degradation reaction of methylene blue in the Fe_2O_3/GSBA-15 photocatalyst under UV light irradiation can be written as Equations (4 – 8).

$$Fe_2O_3 + h\upsilon \rightarrow Fe_2O_3\ (e^- + h+) \quad (4)$$

$$OH^- + h^+ \rightarrow OH^* \quad (5)$$

$$H_2O + h^+ \rightarrow OH^* + H^+ \quad (6)$$

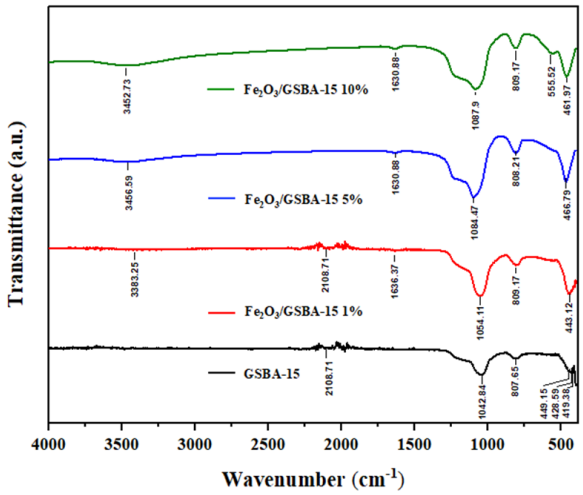

Figure 3. FTIR spectra of gelatin mesoporous silica (GSBA-15) before and after iron oxide incorporation

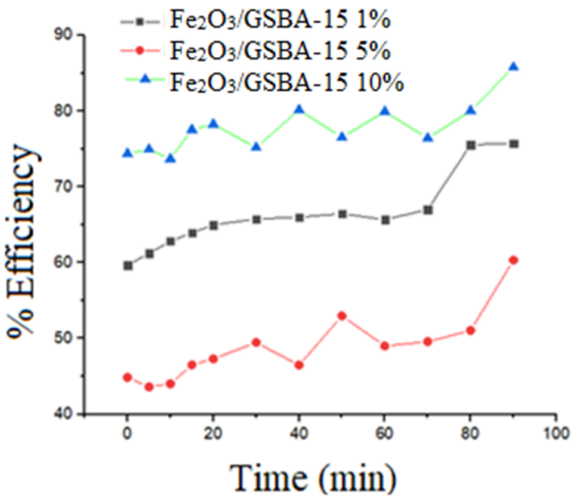

Figure 5. Effect of irradiation time on the degradation efficiency of methylene blue

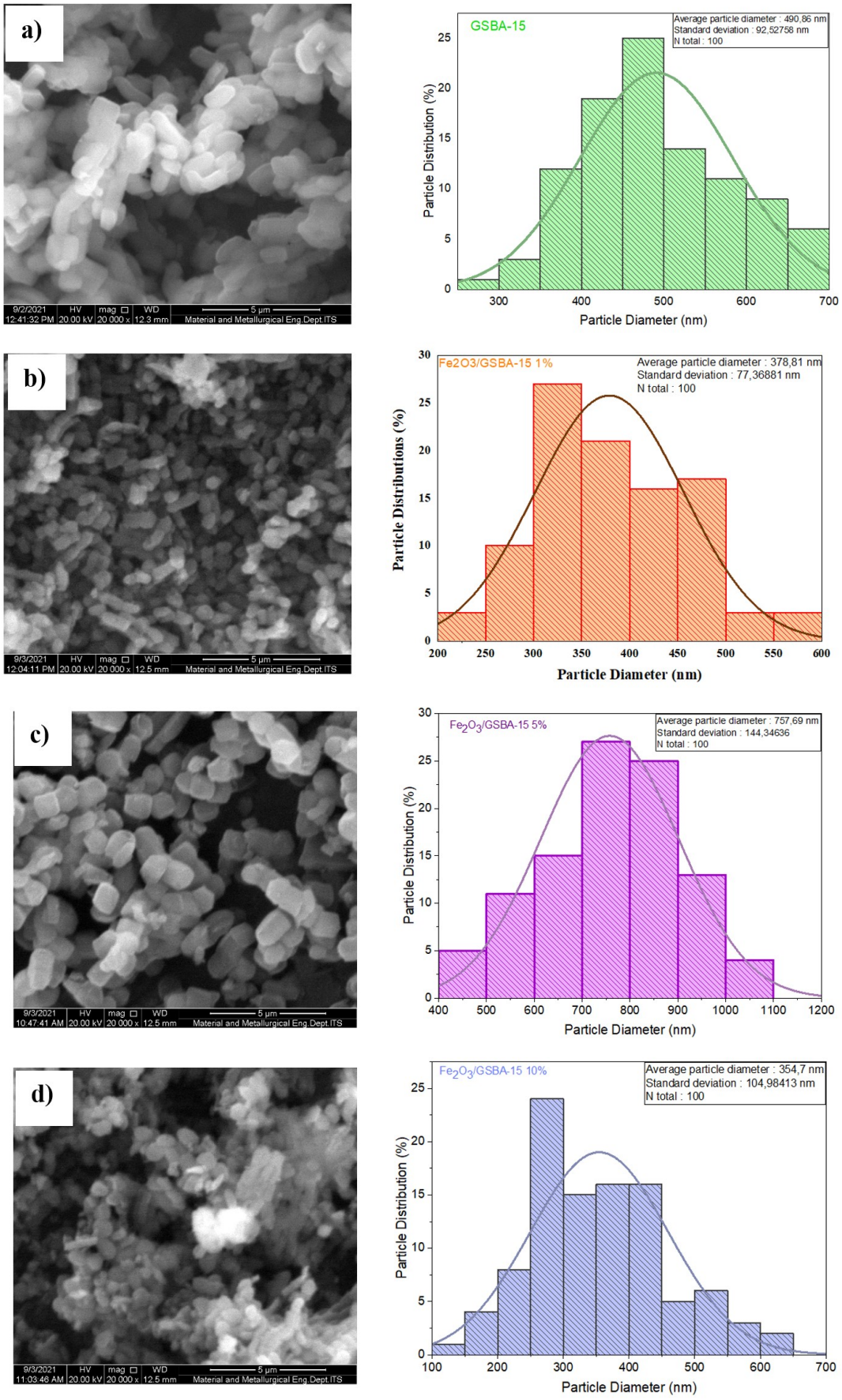

Figure 4. SEM images and particle size distribution of gelatin mesopores silica GSBA-15 before and after iron oxide incorporation

$$OH + \text{Methylene Blue} \rightarrow CO_2 + H_2O \quad (7)$$

$$\text{Methylene Blue} + e^- \rightarrow CO_2 + H_2O \quad (8)$$

Equations (4-8) indicate that when the Fe_2O_3/GSBA-15 photocatalyst absorbs photons with energy equal to or greater than the band gap energy of Fe_2O_3, the electrons in Fe_2O_3 are excited from the valence band to the conduction band. When iron is incorporated into the silica surface [31], holes and electron pairs can be generated. Then, e^- and h^+ can migrate to the surface of Fe_2O_3/GSBA-15 and will enter into a redox reaction with organic pollutants, in this case, methylene blue, on the surface. Holes and electron pairs will react with H_2O or OH^- to produce hydroxyl radicals. These radicals are powerful oxidizing agents and the main oxidizer in the photocatalytic oxidation of methylene blue to carbon dioxide, water, and other mineralized products. Meanwhile, electrons will react with methylene blue to produce reduced products, namely CO_2 and H_2O. In general, the iron oxide incorporated in the gelatin mesoporous silica G-SBA-15 reveals good photodegradation performance, making this material a future photocatalyst material.

4. Conclusions

The incorporation of iron oxide onto gelatin mesoporous silica GSBA-15 by the ultrasonication method has been successfully investigated in this work. The uniform dispersion of iron oxide on GSBA-15 as the supporting material was achieved with ultrasonic radiation. FTIR, XRD, and EDX analysis exhibited successful incorporation of 1-10% iron oxide onto GSBA-15 with the distribution particle size ranging from 30 to 70 nm and the iron content of 0.97 – 5.98 %wt. The blocking pore of 1-10% iron oxide reduced surface area from 481 to 385 m^2/g and pore volume by 5%. The study demonstrated an increase in the photocatalytic activity with enhancing methylene blue degradation as the increasing iron oxide concentration. The degradation efficiency reached optimum at ~ 80% on 10% Fe_2O_3/GSBA-15.

Acknowledgments

The author would like to thank the Ministry of Education, Culture, Research, and Technology, Indonesia, for the Fundamental Research scheme (PDUPT) grant with No. 469.1/UN27.22/PT01.03/2022 by Maria Ulfa.

Table 2. Effect of ultrasonication on MB removal efficiency

Sample name	Support	% Fe	Ultra-sonication	Condition	% Eff.	Ref.
MFS	Silica	10	N	15 min DA, 20 min PC	10	[25]
Fe/AC	Carbon	7.5	N	W = 50 mg, Co 0.025 g/L,	40	[26]
		10	N	PC 180 min, add H_2O_2	66	[26]
		12.5	N		45	[26]
		15	N		59	[26]
SiO_2@$FeCo_2O_4$	Fe	66	N	DA = 30 min, PC=15 min, Co = 10 mg/L, W = 20 mg	99	[27]
Si–Al/α-FeOOH	Fe	75	N	W 20 mg, Co 1 g/L, add H_2O_2	72	[28]
Fe_2O_3/ Mesoporus silica	Silica	35	N	W 20 mg, Co 1 g/L, add H_2O_2	80	[29]
Fe_2O_3/GSBA-15	Silica	0.97	Y	PC 90 min, W 50 mg, Co	66	This work
Fe_2O_3/GSBA-15	Silica	1.58	Y	5 ppm	77	This work
Fe_2O_3/GSBA-15		5.98	Y		85	This work
PVC/TiO_2-BSA NC	BSA	Ti 6%	Y	W0.1 g, V100 mL, Co 10 ppm, PC 700 min	94	[20]
WO_3-rGO thin-film	RGO	W 1%	Y	Co 10 ppm, Weight 0.5 mg, V=1 L	88.5	[22]
zeolite-titanate	-	Ti 9.3%	Y	Molecule : Ibuprofen pH: 7 ± 0.2, H_2O_2 concentration: 0.7 mL, sonication time: 100 min, catalyst dose: 150 mL	98.9	[30]

DA: Dark adsorption, PC: Photocatalytic, W: Weight of photocatalyst, Co: Initial concentration, V: Volume of solution

CRediT Author Statement

Conceptualization, M.U.; methodology, M.U and S.A.I.; validation, M.U and S.A.I.; formal analysis, S.A.I and M.U.; investigation, M.U; data curation, M.U and S.A.I.; writing—original draft preparation, M.U. and S.A.I.; writing—review and editing, M.U; visualization, M.U; supervision, M.U..; funding acquisition, M.U. All authors have read and agreed to the published version of the manuscript.

References

[1] Dutt, M.A., Hanif, M.A., Nadeem, F., Bhatti, H.N. (2020). A review of advances in engineered composite materials popular for wastewater treatment. *J. Environ. Chem. Eng*. 8(5), 104073. doi: 10.1016/j.jece.2020.104073

[2] Wu, L., Yu, J.C., Zhang, L., Wang, X., Li, S. (2004). Selective self-propagating combustion synthesis of hexagonal and orthorhombic nanocrystalline yttrium iron oxide. *J. Solid State Chem*. 177(10), 3666–3674. doi: 10.1016/j.jssc.2004.06.020

[3] Dotto, G.L., Santos, J.M.N., Rodrigues, I.L., Rosa, R., Pavan, F.A., Lima, E.C. (2015). Adsorption of Methylene Blue by ultrasonic surface modified chitin. *J. Colloid Interface Sci.* 446, 133–140. doi: 10.1016/j.jcis.2015.01.046

[4] Brossault, D.F.F., McCoy, T.M., Routh, A.F. (2021). Self-assembly of $TiO_2/Fe_3O_4/SiO_2$ microbeads: A green approach to produce magnetic photocatalysts. *J. Colloid Interface Sci.* 584, 779–788. doi: 10.1016/j.jcis.2020.10.001

[5] Iqbal, M., Saeed, A., Zafar, S.I. (2009).. FTIR spectrophotometry, kinetics and adsorption isotherms modeling, ion exchange, and EDX analysis for understanding the mechanism of Cd^{2+} and Pb^{2+} removal by mango peel waste. *J. Hazard. Mater.* 164(1), 161–171. doi: 10.1016/j.jhazmat.2008.07.141

[6] Ulfa, M., Al Afif, H., Saraswati, T.E., Bahruji, H. (2022). Fast Removal of Methylene Blue via Adsorption-Photodegradation on TiO_2/SBA-15 Synthesized by Slow Calcination. *Materials (Basel).* 15(5471), 1–13.

[7] Ulfa, M., Prasetyoko, D., Bahruji, H., Nugraha, R.E. (2021). Green Synthesis of Hexagonal Hematite (α-Fe_2O_3) Flakes Using Pluronic F127-Gelatin Template for Adsorption and Photodegradation of Ibuprofen. *Materials (Basel)*. 14 (6779), 1–18. DOI: 10.3390/ma14226779

[8] Sugrañez, R., Balbuena, J., Cruz-Yusta, M., Martín, F., Morales, J., Sánchez, L. (2015). Efficient behavior of hematite towards the photocatalytic degradation of NOx gases. *App. Catal. B Environ.* 165(X), 529–536. doi: 10.1016/j.apcatb.2014.10.025

[9] Wu, X., Xie, X., Cao, Y. (2016). Self-magnetization of pyrite and its application in flotation. *Trans. Nonferrous Met. Soc. China*. 26(12), 3238–3244. doi: 10.1016/S1003-6326(16)64456-4

[10] Wang, K., Chen, H., Zhang, X., Tong, Y., Song, S., Tsiakaras, P. (2020). Iron oxide@graphitic carbon core-shell nanoparticles embedded in ordered mesoporous N-doped carbon matrix as an efficient cathode catalyst for PEMFC. *Appl. Catal. B Environ.* 264, 118468. doi: 10.1016/j.apcatb.2019.118468

[11] Si-Hwa, L., Moumita, K., Jung-Hwan, O., Palanichamy, S., Sung-Ho, P., Yun-Sung, L., Il-Kwon, O. (2017). Nanohole-structured, iron oxide-decorated and gelatin-functionalized graphene for high rate and high capacity Li-Ion anodes. *Carbon*. 119, 355–364. 2017. doi: 10.1016/j.carbon.2017.04.031

[12] An, J., Gou, Y., Yang, C., Hu, F., Wang, C. (2013). Synthesis of a biocompatible gelatin functionalized graphene nanosheets and its application for drug delivery. *Mater. Science. Eng. C*. 33(5), 2827–2837. doi: 10.1016/j.msec.2013.03.008

[13] Ulfa, M., Trisunaryanti, W., Falah, I.I., Kartini, I. (2018). Wormhole-Like Mesoporous Carbons from Gelatine as Multistep Infiltration Effect. *Indones. J. Chem*. 16(3), 239-242. doi: 10.22146/ijc.21137

[14] Ulfa, M., Prasetyoko, D., Mahadi, A.H., Bahruji, H. (2020). Size tunable mesoporous carbon microspheres using Pluronic F127 and gelatin as co-template for removal of ibuprofen. *Science. Total Environ.* 711, 135066. doi: 10.1016/j.scitotenv.2019.135066

[15] Ulfa, M., Saraswati, T.E., Mulyani, B., Prasetyoko, D. (2019). Transformation of Iron Nitrate Into Nano Iron Particles. *Journal of Chemical Technology and Metallurgy*. 54(4), 709 – 714.

[16] Mallakpour, S., Azadi, E. (2020). Chapter 11 – Sonochemical protocol for the organosynthesis of TiO_2 and its hybrids: Properties and applications. Inamuddin, Rajender Boddula, Abdulah M. Asiri (Editors) *Green Sustainable Process for Chemical and Environmental Engineering and Science.* Amsterdam: Elsevier. doi: 10.1016/b978-0-12-819540-6.00011-5

[17] Gupta, N.K., Bae, J., Kim, S., Kim, K.S. (2021). Fabrication of Zn-MOF/ZnO nanocomposites for room temperature H_2S removal: Adsorption, regeneration, and mechanism. *Chemosphere*. 274, 129789. doi: 10.1016/j.chemosphere.2021.129789

[18] Malika, M., Sonawane, S.S. (2021). Statistical modeling for the Ultrasonic photodegradation of Rhodamine B dye using aqueous based Bimetal doped TiO_2 supported montmorillonite hybrid nanofluid via RSM. *Sustain. Energy Technol. Assessments*. 44, 100980. doi: 10.1016/j.seta.2020.100980

[19] Kuterasiński, L., Filek, U., Gackowski, M., Zimowska, M., Ruggiero-Mikołajczyka, M., Jodłowski, P.J. (2021). Ultrasonics Sonochemistry Sonochemically prepared hierarchical MFI-type zeolites as active catalysts for catalytic ethanol dehydration. *Ultrasonics Sonochemistry*. 74, 105581. doi: 10.1016/j.ultsonch.2021.105581

[20] Mallakpour, S., Shamsaddinimotlagh, S. (2018). Ultrasonics - Sonochemistry Ultrasonic-promoted rapid preparation of PVC/TiO_2-BSA nanocomposites: Characterization and photocatalytic degradation of methylene blue. *Ultrasonic Sonochemistry*. 41, 361–374. doi: 10.1016/j.ultsonch.2017.09.052

[21] Zhang, S., Zhang, Y., Li, Z. (2018). Ultrasonic monitoring of setting and hardening of slag blended cement under different curing temperatures by using embedded piezoelectric transducers. *Constr. Builds. Mater.* 159, 553–560. doi: 10.1016/j.conbuildmat.2017.10.124

[22] Dhivyaprasath, K., Wiston, B.R., Preetham, M., Harinee, S., Ashok, M. (2021). Ultrasonic spray deposition of WO_3-rGO thin-film composite for photocatalytic degradation of methylene blue. *Optics (Stuttg).* 244, 167593. doi: 10.1016/j.ijleo.2021.167593

[23] Ulfa, M., Setiarini, I. (2022). The Effect of Zinc Oxide Supported on Gelatin Mesoporous Silica (GSBA-15) on Structural Character and Their Methylene Blue Photodegradation Performance. *Bull. Chem. React. Eng. Catal.* 17(2), 363–374. doi: 10.9767/bcrec.17.2.13712.363-374

[24] Lu C., Zhang S., Wang J., Zhao X., Zhang L., Tang A. (2022). Efficient activation of peroxymonosulfate by iron-containing mesoporous silica catalysts derived from iron tailings for the degradation of organic pollutants. *Chem. Eng. J.* 446(P1), 137044. doi:10.1016/j.cej.2022.37044

[25] Silva, L.A., Borges, S.M.S., Paulino, P.N., Fraga, M.A., Oliva, S.T., Marchetti, S.G., Rangel, M.C. (2017). Methylene blue oxidation over iron oxid...vated carbon derived from peanut hulls. *Catal. Today*. 289, 237–248. DOI: 10.1016/j.cattod.2016.11.036

[26] Maniyazagan, M., Naveenkumar, P., Yang, H.W., Zuhaib, H., Kang, W.S., Kim, S.J. (2022). Hierarchical SiO_2@$FeCo_2O_4$ core-shell nanoparticles for catalytic reduction of 4-nitrophenol and degradation of methylene blue. *J. Mol. Catal. A Chem.*, 365, 120–123. doi: 10.1016/j.molliq.2022.120123

[27] Yuan, B., Xu, J., Li, X., Fu, M.L. (2013). Preparation of Si–Al/α-FeOOH catalyst from an Iron-Containing Waste Surface-Catalytic Oxidation of Methylene Blue at Neutral pH Value in the Presence of H_2O_2. *Chem. Eng. J.* 226, 181–188. DOI: 10.1016/j.cej.2013.04.058

[28] Coelho, J.V., Guedes, M.S., Prado, R.G., Tronto, J., Ardisson, J.D., Pereira, M.C., Oliveira, L.C.A. (2014). Effect of iron precursor on the Fenton-like activity of Fe_2O_3/mesoporous silica catalysts prepared under mild conditions. *Appl. Catal. B Environ.*, 144, pp. 792–799, 2014. doi: 10.1016/j.apcatb.2013.08.022

[29] Hitam, C.N.C., Jalil, A.A., Izan, S.M., Hassim, M.H., Chanlek, N. (2020). The unforeseen relationship of Fe_2O_3 and ZnO on fibrous silica KCC-1 catalyst for fabricated Z-scheme extractive-photooxidative desulphurization. *Powder Technol.* 375, 397–408. doi: 10.1016/j.powtec.2020.07.114